0026-895X/04/6601-70–75
MOLECULAR PHARMACOLOGY
U.S. Government work not protected by U.S. copyright
Mol Pharmacol 66:70–75, 2004

Vol. 66, No. 1
1906/1153252
Printed in U.S.A.

In Silico Simulation of Inhibitor Drug Effects on Nuclear Factor-κB Pathway Dynamics

Myong-Hee Sung and Richard Simon

Biometric Research Branch, National Cancer Institute, National Institutes of Health, Bethesda, Maryland

Received February 3, 2004; accepted April 2, 2004

This article is available online at http://molpharm.aspetjournals.org

ABSTRACT

NF-κB is a transcription factor family that activates numerous genes that are related to cell survival, apoptosis, and cell migration. Its persistent activity is associated with tumor formation, growth, metastasis, and drug resistance in many cancer types, including lymphoma, colon cancer, and breast cancer. Current therapeutic efforts for inhibiting this central "switch" include using small molecules to block a selected target in this pathway. Recognizing the regulatory network structure of the NF-κB pathway, we examine in silico the effects of inhibitors targeting various network components, using a kinetic model of the pathway. By simulating the corresponding perturbed system dynamics, we show the resulting time course of inhibition has distinct target-specific profiles. In particular, greater oscillatory potential exists for inhibition of upstream events than for direct inhibition of NF-κB, at low drug concentrations. This phenomenon is observed also when we examine the dynamic effects of the recently approved proteasome inhibitor, bortezomib (PS-341), and compare it with other inhibitors, taking its pharmacokinetics into consideration. Such kinetic analyses of the "drugged" molecular system will facilitate optimal drug target selection and the development of treatment protocols for a molecularly targeted therapy.

Nuclear factor (NF)-κB family of proteins is considered a central regulator of cellular responses to various conditions, such as infections, hypoxia, growth factors, and physical stress. Generally eliciting pro-survival/antiapoptotic gene expression programs, NF-κB is typically expressed transiently to activate certain target genes (Pahl, 1999). Under normal conditions, it is kept in the cytoplasm by the inhibitor proteins IκB. When an upstream stimulus activates IκB kinase (IKK), it phosphorylates IκB, which will then be degraded in a ubiquitin-proteasome pathway. Thereafter, released NF-κB proteins translocate into the nucleus and activate the transcription of target genes. NF-κB also activates its own inhibitor, IκBα, giving rise to a negative feedback control (Ghosh and Karin, 2002).

The activity of NF-κB is constitutively elevated in many types of cancer, promoting the growth and progression of tumors and resistance to chemotherapy (Darnell, 2002; Garg and Aggarwal, 2002). As a result, the NF-κB pathway has emerged as an attractive drug target. Small molecules that disrupt this pathway are currently being evaluated for therapeutic purposes (Ni et al., 2001; Darnell, 2002; Garg and Aggarwal, 2002; Hideshima et al., 2002; Orlowski and Baldwin, 2002). Selection of drug targets within the NF-κB pathway should take into consideration the network structure of this activation pathway, which minimally consists of IKK, IκBα, and NF-κB, and their interconnected dynamic interactions. Choosing the optimal point of inhibition can be facilitated by kinetic analyses of this activation module.

In this study, we use a quantitative dynamic model for the purpose of analyzing the changes that may arise from therapeutic modulations. This is an attempt to integrate different types of biological data to construct a working model that is predictive of the drug effects upon the targeted molecular network (Sarkar and Lauffenburger, 2003). The goal is to assess different therapeutic strategies and treatment schedules, using quantitative dynamical models and preclinical data, and select clinical protocols that maximize the desired drug effect. Such models should include not only the network dynamics of the target molecular system but also a profile of the drug concentration and proposed mechanism(s) of the drug action. Consequences of a particular perturbation can be simulated in time course using a system of differential equations that describes the model. Hoffmann et al. (2002) recently constructed a differential equations model of the NF-κB pathway using published reaction parameters and applied it to analyze the response patterns to various input signals. In this study, we combine a similar model for the NF-κB network with intracellular concentration models for various types of inhibitors and illustrate potential utilities of such systems analyses for clinical studies.

Materials and Methods

Model Construction. To understand the simultaneous interactions of various molecular species in the NF-κB activation module,

ABBREVIATIONS: NF, nuclear factor; IKK, IκB kinase; PK, pharmacokinetics; AUIC, area under the inhibition curve.

An erratum has been published:
http://molpharm.aspetjournals.org/content/66/3/770.full.pdf

we modeled this dynamical system using a set of ordinary differential equations and mass action kinetics (see Fig. 1). The reaction parameters were obtained from Hoffmann et al. (2002). These parameters are experimentally observed values that were either directly measured or indirectly estimated. We did not consider the effects of inhibitor proteins IκBβ or IκBε because, under constitutive activity of IKK, NF-κB does not directly induce resynthesis of these proteins, so their presence becomes negligible in the steady state. The processes involved in gene transcription and translation are very complex with mostly unknown kinetic features. Modeling those individual steps is not necessary as long as none of these intermediates interact with the other model components. For our purpose, this was indeed the case, because modulating the transcription/translational machineries would not be specific to the NF-κB system and hence outside of our focus on highly specific therapies. Therefore, we modeled de novo synthesis of IκBα as a single delayed process. This process appears in the model as a first-order term with rate constant that was calibrated so that the temporal profiles of NF-κB activity and IκB qualitatively match the experimental data. The time delay between the NF-κB binding to the promoter DNA and the appearance of synthesized functional IκBα proteins in the cytoplasm was set at 40 min. Changing this value within a realistic range affects the period of the oscillation but does not alter the qualitative dynamical features of the system.

Simulation Protocol. The initial condition for the unstimulated system (no IKK activation) was 0.03 μM free cytoplasmic IκBα; 0.04 μM cytoplasmic complex NF-κB:IκBα; free nuclear IκBα. The onset of IKK activity was introduced at $t = 0$ as a Gaussian spike $k(t)$ in *d/dt* IKK (see Fig. 1) with total influx of 0.025 μM. All simulations were run using MATLAB (release 13), which has a delay differential equations solver, "dde23".

The molecule A was assumed to competitively inhibit IKK with binding kinetics the same as that of the natural reaction involving NF-κB:IκBα and IKK. The degradation of this molecule was assumed to be negligible to reflect the kinetics of an unnatural synthetic molecule. The introduced concentrations for Fig. 4, A and B, were 50 and 150 nM, respectively. Equations for A and for the complex A-IKK were added to the constitutive NF-κB model constructed above. In addition, a term was added to the IKK equation for interaction between A and IKK. The mass action association/dissociation rate constants were a_2 and d_2 based on the assumptions. Several other concentration values of A were also simulated to see the effect on the overall dynamics.

The effect of administering the molecule B is modeled in a similar manner as for A. Molecule B competitively inhibits cytoplasmic NF-κB with the same binding kinetics as the reaction between NF-κB and IκBα (with rate constants a_1 and d_1). Because nuclear translocation of B was not allowed, it could not inhibit nuclear NF-κB.

For simulating the inhibition of the degradation of IκBα, we could not introduce an additional component to the system as A or B above because the degradation processes were not explicit in the model. Instead, we adjusted the term for NF-κB released after the degradation of IκBα, and the individual terms for IκBα and NF-κB:IκBα molecules rescued from degradation. More specifically, r_1 NF:I:IKK was changed to 0.2 r_1 NF:I:IKK for *d/dt* F, d_3 I:IKK to (d_3 + 0.8 r_2) I:IKK for *d/dt* I, and d_2 NF:I:IKK to (d_2 + 0.8 r_1) NF:I:IKK for *d/dt* NF:I. These adjustments corresponded to the 80% inhibition in the rate of degradation. A separate simulation was run for 95% inhibition.

To simulate the inhibition dynamics under a pharmacokinetic (PK) profile of drug concentration, data on the proteasome inhibitor bortezomib were used. Ideally, the drug input to the molecular pathway should be the drug concentration measured from isolated cancer cells. For many reasons, however, such a data collection is rare. In the absence of such data on bortezomib, we used a coarse approximation from conventional PK data. Published pharmacodynamics data for intravenously administered PS-341 (bortezomib) report 60% blood proteasome inhibition at 1 h after dosing as the maximum inhibition point (Orlowski et al., 2002). The mean half-life of bortezomib (also known as Velcade) is stated to range from 9 to 15 h in the prescribing information by Millennium Pharmaceuticals, Inc (http://www.mlnm.com/products/velcade/full_prescrib_velcade.pdf). Based on these data, we used a simple PK model in which the drug concentration increases linearly up to the maximum level at 1 h and decays exponentially with a half-life of 12 h. This PK model was used also for molecules A and B to compare the drug effects based on equal PK profiles. The maximum drug levels were 60% inhibition, 50 nM, and 50 nM for bortezomib, molecule A, and molecule B, respectively.

Results

We focused on situations in which IKK was constitutively active, even though the method could be generalized to other situations. As in Hoffmann et al. (2002), NF-κB in this work mainly represents the common p65:p50 heterodimer. Fig. 2 describes the basic NF-κB model and the three types of inhibitors considered in this article. Figure 3 shows the time course of the various proteins where constant IKK activity is introduced at $t = 0$ after which the system reaches a steady state. We have examined three inhibition strategies and sim-

$$\frac{dNF}{dt} = -a_1 NF \cdot I + d_1 NF:I + r_1 NF:I:IKK + dg_2 NF:I - i_{NF} NF + e_{NF} NF_n$$

$$\frac{dI}{dt} = -a_1 NF \cdot I + d_1 NF:I - a_3 I \cdot IKK + d_3 I:IKK + sNF_n(t-\tau) - dg_1 I - i_I I + e_I I_n$$

$$\frac{dNF:I}{dt} = a_1 NF \cdot I - d_1 NF:I - a_2 (NF:I) \cdot IKK + d_2 NF:I:IKK - dg_2 NF:I + e_{NF:I} NF_n:I_n$$

$$\frac{dNF_n}{dt} = -a_1 NF_n \cdot I_n + d_1 NF_n:I_n + i_{NF} NF - e_{NF} NF_n$$

$$\frac{dI_n}{dt} = -a_1 NF_n \cdot I_n + d_1 NF_n:I_n + i_I I - e_I I_n$$

$$\frac{dNF_n:I_n}{dt} = a_1 NF_n \cdot I_n - d_1 NF_n:I_n - e_{NF:I} NF_n:I_n$$

$$\frac{dIKK}{dt} = k(t) - a_2 (NF:I) \cdot IKK + (d_2 + r_1) NF:I:IKK - a_3 I \cdot IKK + (d_3 + r_2) I:IKK$$

$$\frac{dI:IKK}{dt} = a_3 I \cdot IKK - (d_3 + r_2) I:IKK$$

$$\frac{dNF:I:IKK}{dt} = a_2 (NF:I) \cdot IKK - (d_2 + r_1) NF:I:IKK$$

Fig. 1. A kinetic model of NF-κB. The system of ordinary differential equations describes the reaction network of the NF-κB activation module. *NF* and *I* represent concentrations of NF-κB and IκBα, respectively. Consecutively written molecules connected with a colon represent complexes; e.g., *NF:I* is the complex of NF-κB and IκBα. Nuclear proteins are specified by the subscripted letter *n*; e.g., *NFn* is nuclear NF-κB. Lowercase symbols are kinetic parameters whose values were adapted from Hoffman et al. (2002), except for the IκBα synthesis-related parameters s and τ (see *Materials and Methods*).

ulated the resulting "inhibition dynamics". The following analysis can be tailored to any small molecule inhibitors and treatment protocols.

Our first example was for a molecule A, which competitively inhibited IKK. We assumed that the interaction kinetics was as efficient as that between IKK and NF-κB:IκBα. In particular, the association/dissociation constants were the same for the two reactions, making A an "equal" competitor. Figure 4 shows the time course of the proteins when the molecule was introduced at a steady state of the constitutively active NF-κB system shown previously. Two concentrations of A were chosen to represent the differential dynamics corresponding to low and high drug doses. It was striking that drug administration with a low dose resulted in a highly oscillatory behavior of the system even if the active IKK level was reduced significantly as expected (Fig. 4A). Moreover, this behavior was typical for a range of low concentrations of the inhibitor A. Higher doses gradually diminished the spikes of nuclear NF-κB until the system exhibited a damped oscillation at a much higher dose of A (Fig. 4B).

Another scenario was to block the degradation pathway of IκBα after it is phosphorylated by IKK. This could be achieved by inhibiting ubiquitination of IκBα or its degradation by the 26S proteasome. Inhibiting 80% of the degradation rate resulted in oscillation of the system in a similar manner to that in the example above (Fig. 4A). As the inhibition efficiency was increased, the oscillation shifted into a

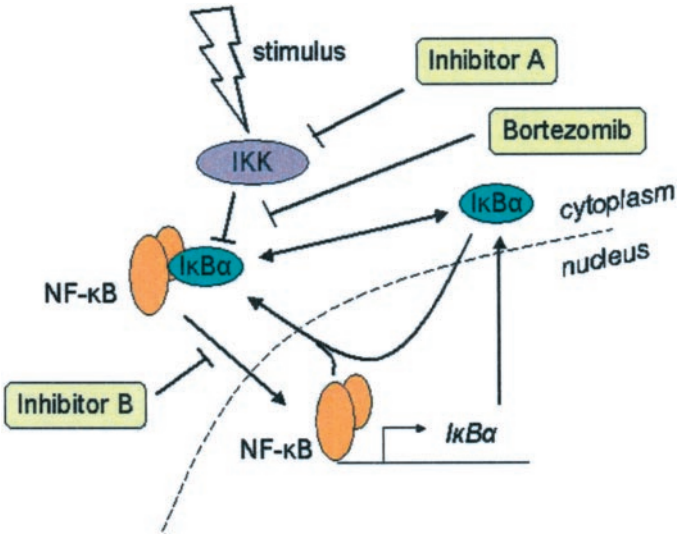

Fig. 2. NF-κB regulatory network structure. A pathway model for NF-κB is shown with the three inhibitors considered in the text. Upstream stimuli converge at IKK and active IKK phosphorylates IκB proteins that are subsequently degraded by the ubiquitin-proteasome pathway (not shown here). Freed from IκB, NF-κB then enters the nucleus to activate transcription of target genes. IκBα is also induced by NF-κB and newly synthesized IκBα proteins can bind to NF-κB in the cytoplasm or translocate into the nucleus and shuttle NF-κB back from the nucleus. Inhibitor A binds to active IKK so that enzymatic activity of IKK is blocked. Inhibitor B binds to free NF-κB in the cytoplasm blocking its nuclear entry. The inhibitor bortezomib (Velcade) blocks the activity of the proteasome that degrades IκBα.

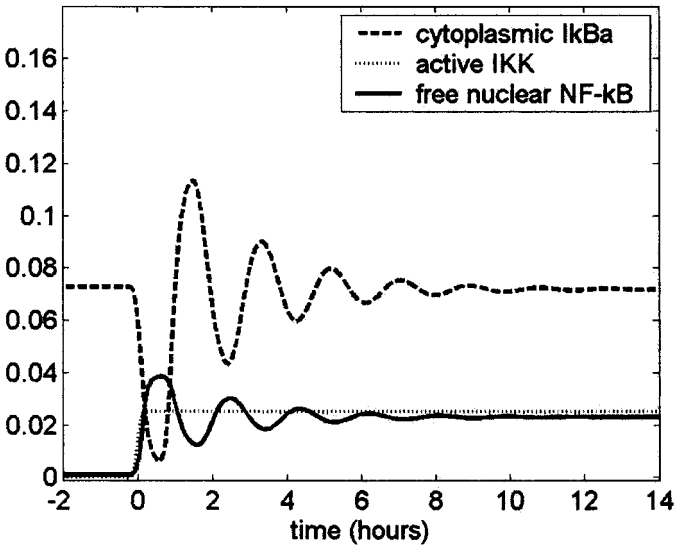

Fig. 3. A constitutively active NF-κB system. A constant level of active IKK is added to the system at $t = 0$. In several hours, the system reaches a steady state of constitutive NF-κB activity. The curves correspond to concentrations of cytoplasmic IκBα, active IKK, and free nuclear NF-κB. The concentration unit for all plots in this article is micromolar.

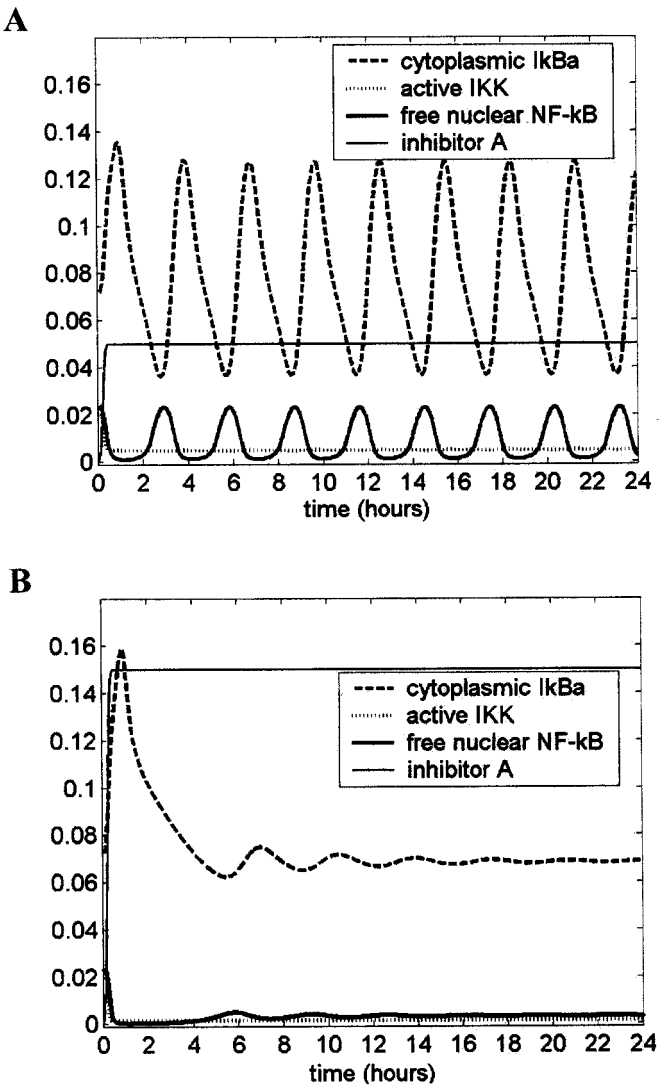

Fig. 4. Competitive inhibition of IKK. An inhibitor molecule A was introduced to the steady state in Fig. 3 to block the constitutive activity of NF-κB by targeting the active IKK. The molecule inhibited IKK phosphorylation of IκBα by competitively binding to IKK. The inhibitor concentrations were 0.05 μM (A) and 0.15 μM (B). All subsequent plots follow a similar scheme.

damped oscillation. Inhibiting 95% of the degradation rate resulted in an inhibition dynamics very similar to that shown in Fig. 4B. The time course plots looked virtually identical to the corresponding plots in Fig. 4 for low and high inhibition cases. The proteasome inhibitor, bortezomib (PS-341), which was recently approved by the FDA for the treatment of multiple myeloma, acts by inhibiting the 26S proteasome (Adams et al., 1999; Orlowski et al., 2002). Because this proteasome has additional roles in degrading proteins that are involved in cell cycle control, antigen presentation, and other processes, bortezomib modulates a variety of cellular processes that may contribute to toxicity. In this regard, it is a challenge in reality to achieve even 65% inhibition of the proteasome without exceeding the maximum tolerated dose (Orlowski et al., 2002).

The last inhibition approach was competitive inhibition of NF-κB itself in the cytoplasm. The inhibitor molecule (B) was assumed to have the same association/dissociation constants as for the interaction between NF-κB and IκBα, making it equally competent in binding to NF-κB. Figure 5 shows the time course of the system showing stable reduction of the level of nuclear NF-κB after some initial oscillation. It is interesting that the high concentration of the inhibitor B drove the system more into oscillation. The system eventually reached a steady state but the oscillation lasted significantly longer than it did in low-dose inhibition. This observation may reflect the fact that we assumed the binding capacity of the molecule B was the same as IκBα, which made possible the dynamic exchange of NF-κB between its natural inhibitor and its synthetic inhibitor. The oscillation was present at both dose levels but became more pronounced when the system was perturbed with higher magnitude.

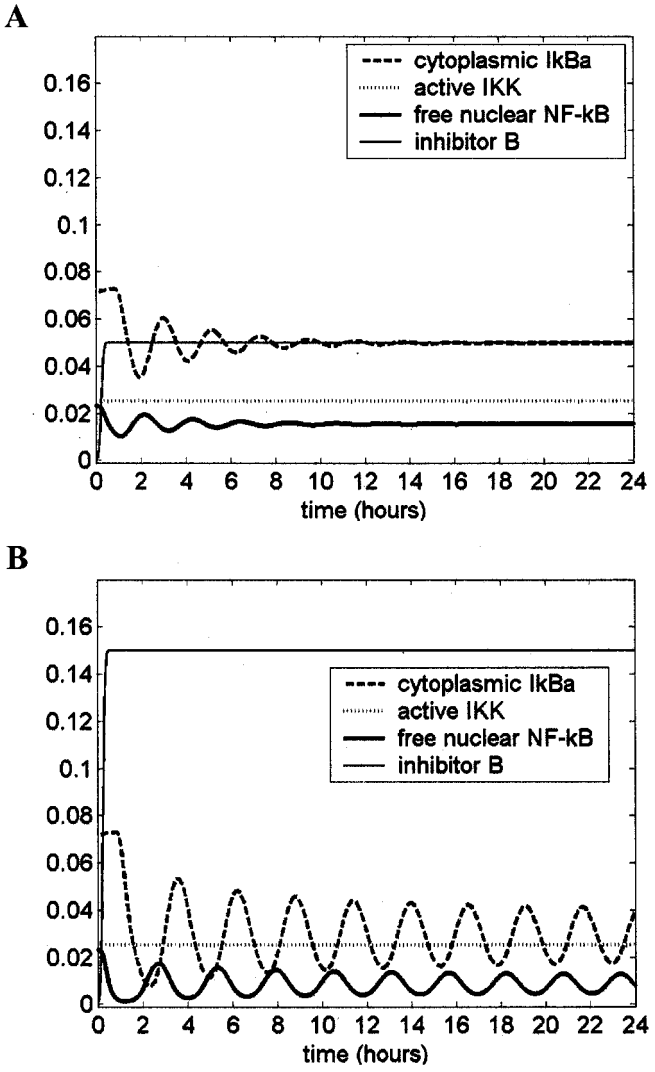

Fig. 5. Competitive inhibition of cytoplasmic NF-κB. Inhibitor molecule B targets free cytoplasmic NF-κB directly by competitive binding. Therefore, NF-κB cannot translocate to the nucleus and activate target gene transcription. The inhibitor concentrations were 0.05 μM (A) and 0.15 μM (B).

Next, we compared the above three in the context of transient intracellular drug kinetics. Although pharmacokinetics (usually measured as plasma drug concentration) and intracellular drug concentration kinetics in target cells should be distinguished in ideal situations, here we took common first-order pharmacokinetics as a proxy for the target intracellular drug concentration, because of lack of more detailed data. Because bortezomib is currently the only inhibitor of NF-κB activation with known mechanism of action and pharmacokinetics (http://www.mlnm.com/products/velcade/full_prescrib_velcade.pdf,), we took its pharmacokinetics as an intracellular "wave" after a single dose administration of the inhibitors. This allowed a pharmacokinetically more realistic yet unbiased comparison of the different targeted approaches. In this setting, it was consistently observed that the first two approaches (using molecule A or bortezomib) produced virtually identical system dynamics (i.e., highly oscillatory), whereas inhibiting cytoplasmic NF-κB (using molecule B) resulted in stable reduction of the target, nuclear NF-κB. Figure 6A shows the inhibition dynamics where the pharmacodynamics of bortezomib reached maximum proteasome inhibition of 60% at 1 h after drug administration and decayed with a half-life of 12 h (see *Materials and Methods*). Figure 6, B and C, corresponds to the pharmacokinetics of inhibitors A and B, respectively, with maximum concentration of 50 nM and half-life of 12 h.

To facilitate comparison of different inhibitors of the same pathway, we defined the area under the inhibition curve (AUIC) as the area under the percentage of inhibition versus time curve during a single dose interval, which is a measure of total drug effect from a single dose. This concept mirrors the area under the drug concentration curve in pharmacokinetics. Because the dose interval was arbitrarily set to be 24 h here, we scaled AUIC by dividing by 24 h so that this quantity was the same as the mean percentage of inhibition over the interval. Hence, we could use the formula AUIC = [1 − mean (NF_n)/(steady state NF_n in the absence of drug)] × 100 (%), where NF_n is the concentration of free nuclear NF-κB.

We considered several situations to conduct AUIC comparison analysis of various therapeutic strategies with the three types of inhibitors. The AUIC values depend on characteristic properties of the inhibitors such as the target-binding affinities and their PK. For inhibitors A, B, and bortezomib, the scaled AUIC values were 40.3%, 20.1%, and 19.6%, respectively, from the simulations in Fig. 6. We have to keep in mind that, for A and B, the drug properties were based on our assumptions because of the lack of actual data. For example, the maximum tolerated dose of an IKK inhibitor or an NF-κB inhibitor might be substantially higher than that of a proteasome inhibitor (e.g., bortezomib) because the former type of inhibition is thought to be more NF-κB-specific and might

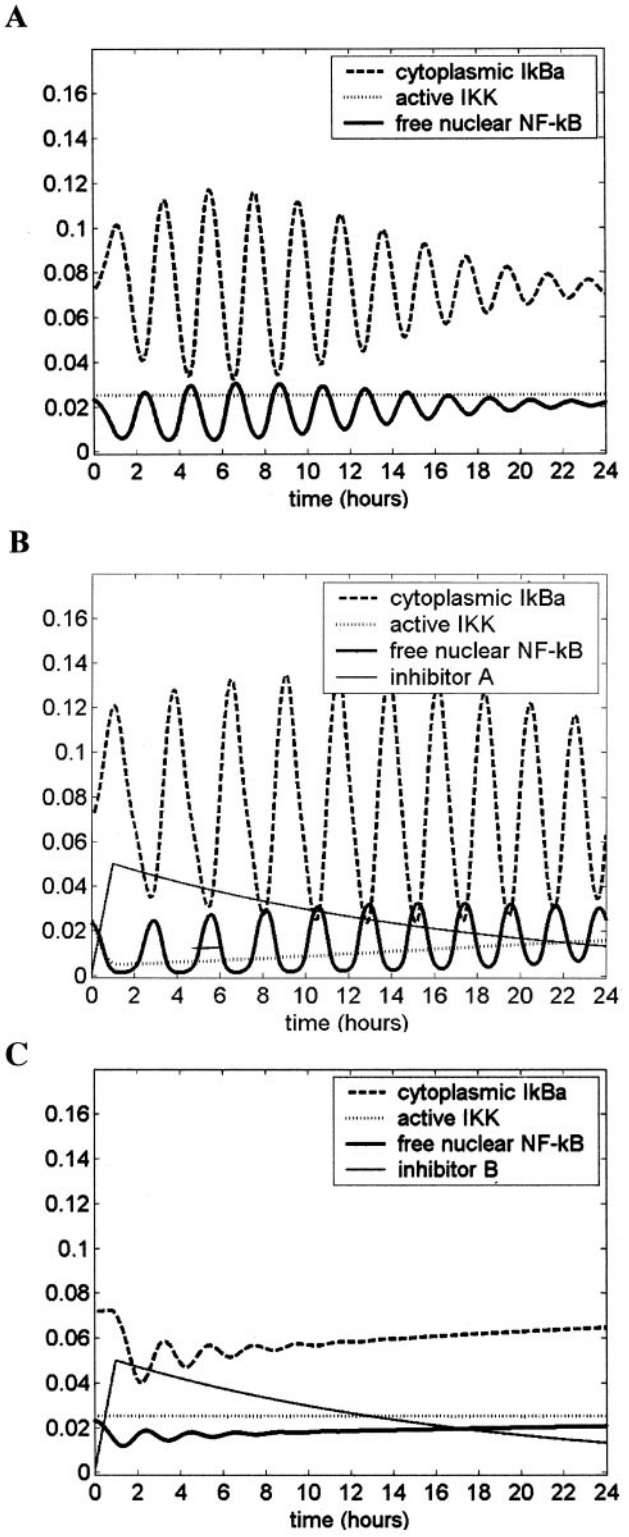

Fig. 6. Inhibition of NF-κB activation when all inhibitors follow the pharmacokinetics of bortezomib (PS-341). The inhibition dynamics was examined using the pharmacokinetics of bortezomib, for the inhibitor of the 26 S proteasome (A), inhibitor A (B), and inhibitor B (C). A standard pharmacokinetic model was constructed using the maximum inhibition point and the half-life of bortezomib (see *Materials and Methods*). Each inhibitor was introduced at $t = 0$, reached the maximum level after 60 min, and decayed with half-life of 12 h. The time courses are shown up to 24 h after drug administration. Our model does not have the proteasome as an explicit model component. Instead, the drug effects are represented implicitly by altered equation terms. Therefore, a curve for bortezomib is not drawn in A.

produce less toxicity. In addition, it may be possible to enhance the drug affinity to the target molecule by using the structural information of the drug-target interface, if available. Therefore, we varied the maximum drug concentration (achieved at 1 h after dosing) and the drug binding affinity to assess their effects on the AUIC. Table 1 summarizes the simulation results for the various strategies. Even when the maximum drug activity was set at 100% inhibition, bortezomib could reach an AUIC of only 39.9%. The AUIC could be increased significantly by either higher doses or higher target-binding affinities, as expected. However, the impact of a given increase in dose or binding affinity was much greater for inhibitors targeting the kinase IKK (A) than for those targeting the proteasome or NF-κB itself (B). If the comparison were applied to inhibitors whose actual properties are known, the AUIC values could be used to select the most effective therapeutic agent.

Discussion

Our simulations suggest that the system behaves differently depending on which molecule is targeted for inhibition within the pathway. In particular, inhibition of the upstream events (IKK activity and IκBα degradation) produced similar inhibition dynamics, whereas direct inhibition of NF-κB resulted in a distinct dynamics. This is in contrast to the simplistic view of static inhibition. The inhibition dynamics depends on the specific target of inhibition and the intracellular concentration of the inhibitor molecule. Short transient spikes in the level of nuclear NF-κB in an oscillating system (e.g., from inhibiting upstream events with a low drug dose) may be enough to trigger discrete bursts of the expression of some immediate target genes. The consequences of this could be best considered in the context of particular tumor cell types. In the examples of upstream blockade, complete inhibition may be achieved only if the intracellular concentration of the drug is high, perhaps unrealistically so. Therefore, high oscillation of the system might be inevitable for a subset of the cancer cells with low drug concentration. One might attempt to overcome this partial inhibition by modifying the drug dose and schedule. This kind of partial inhibition seems to be less pronounced for drugs targeting NF-κB directly, as suggested by the model. The oscillation is milder both for high and low drug concentrations.

Transient or prolonged oscillations are inevitable conse-

TABLE 1
AUIC comparison of various therapeutic situations

Inhibitor Type	Maximum Concentration or Activity (% Inhibition)	Binding Affinity	AUIC
		nM	%
A	50 (nM)	6.8[a]	22.5
	150 (nM)	6.8	40.3
	50 (nM)	0.68	67.6
B	50 (nM)	1[a]	20.1
	150 (nM)	1	44.7
	50 (nM)	0.1	48.2
Bortezomib	60 (%)	N/A	19.6
	100 (%)	N/A	39.9

[a] These values are from the original assumption about binding affinities of inhibitor A and B.

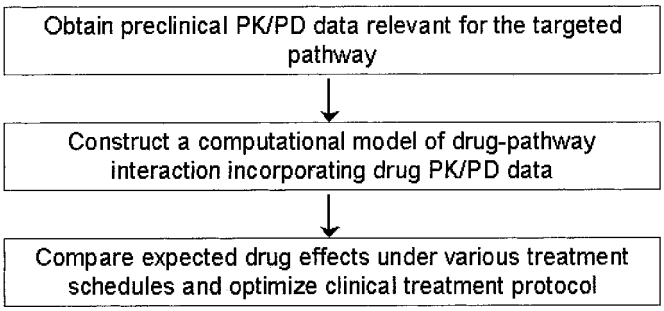

Fig. 7. Proposed utility in clinical research.

quences of any network that possesses robust negative feedback. It is expected to occur when the system moves from one stable state to another (from active to inactive, or vice versa). Because many, if not all, molecular pathways contain such a feature, inhibition attempts of such pathways should also consider this phenomenon and possibly exploit its properties to therapeutic advantages.

The drug concentration in the target cell may have different time course than the first-order pharmacokinetics we used above. However, especially for hematological cancers, the drug concentration may be quite comparable between the plasma and the target cell compartments. For solid tumors, the parallel would be less prominent but the corresponding drug concentrations may still be related after adjusting for delays and distribution, etc. The drug concentrations within tumor cells of treated patients fluctuate according to the pharmacokinetics and penetrability of the drug into the target tissue and cells. The consequence of this variability upon the inhibition dynamics should be examined when assessing drugs that inhibit specific targets in the pathway. The expected modulation estimated by the inhibition dynamics can reveal whether key downstream effector molecules are sufficiently inhibited at all times under various treatment protocol scenarios. The present approach of combining simple pharmacokinetics and a systems model of the target pathway is a compromise taken in the absence of more accurate pharmacokinetic data at a finer cellular resolution.

The AUIC was introduced as a measure of total drug effect of an inhibitor. The AUIC seems to be influenced most strongly by what the drug is targeting within the pathway. Not only can this be used to compare different inhibitors as single agents, but also can it be used to assess synergism/antagonism of combination therapies of inhibitors of the same pathway. For example, if the AUIC for two inhibitors administered together is greater than the sum of the AUIC values for each inhibitor separately, there is benefit in the combination therapy as a result of synergy.

The general approach presented here can facilitate rational strategies for drug development by bridging the gap between the preclinical and clinical stages, as in Fig. 7 for example. The dynamic systems point of view may have useful applications for simultaneously optimizing the drug target, dosage, and treatment schedule. Although not considered in this work, the optimization can also be done such that specified toxicities are minimized. It is critical that therapeutic optimization must be done in light of diverse adjustable parameters including molecular/cellular properties, in vivo PK/pharmacodynamics properties, and dosing schedule of the drug. For this purpose, a quantitative model can be used to link the multiscale parameters of the system. More work should be devoted in the future to make firm links between knowledge gained about disease-related molecular pathways and clinical observations regarding the corresponding targeted therapeutics. In summary, we believe that the analysis of inhibition dynamics is an important emerging tool that should be incorporated into any molecularly targeted therapeutic strategies along with considerations of drug design, synthesis, toxicity, and delivery.

Acknowledgments

We thank Aneil Mallavarapu for locating the pharmacokinetics information of Velcade (bortezomib).

References

Adams J, Palombella VJ, Sausville EA, Johnson J, Destree A, Lazarus DD, Maas J, Pien CS, Prakash S, and Elliott PJ (1999) Proteasome inhibitors: a novel class of potent and effective antitumor agents. *Cancer Res* **59:**2615–2622.

Darnell JE Jr (2002) Transcription factors as targets for cancer therapy. *Nat Rev Cancer* **2:**740–749.

Garg A and Aggarwal BB (2002) Nuclear transcription factor-kappaB as a target for cancer drug development. *Leukemia* **16:**1053–1068.

Ghosh S and Karin M (2002) Missing pieces in the NF-kappaB puzzle. *Cell* 109(Suppl):S81–S96.

Hideshima T, Chauhan D, Richardson P, Mitsiades C, Mitsiades N, Hayashi T, Munshi N, Dang L, Castro A, Palombella V, et al. (2002) NF-κB as a therapeutic target in multiple myeloma. *J Biol Chem* **277:**16639–16647.

Hoffmann A, Levchenko A, Scott ML, and Baltimore D (2002) The IkappaB-NF-kappaB signaling module: temporal control and selective gene activation. *Science (Wash DC)* **298:**1241–1245.

Ni H, Ergin M, Huang Q, Qin JZ, Amin HM, Martinez RL, Saeed S, Barton K, and Alkan S (2001) Analysis of expression of nuclear factor kappa B (NF-kappa B) in multiple myeloma: downregulation of NF-kappa B induces apoptosis. *Br J Haematol* **115:**279–286.

Orlowski RZ and Baldwin AS Jr (2002) NF-kappaB as a therapeutic target in cancer. *Trends Mol Med* **8:**385–389.

Orlowski RZ, Stinchcombe TE, Mitchell BS, Shea TC, Baldwin AS, Stahl S, Adams J, Esseltine DL, Elliott PJ, Pien CS, et al. (2002) Phase I trial of the proteasome inhibitor PS-341 in patients with refractory hematologic malignancies. *J Clin Oncol* **20:**4420–4427.

Pahl HL (1999) Activators and target genes of Rel/NF-kappaB transcription factors. *Oncogene* **18:**6853–6866.

Sarkar CA and Lauffenburger DA (2003) Cell-level pharmacokinetic model of granulocyte colony-stimulating factor: implications for ligand lifetime and potency in vivo. *Mol Pharmacol* **63:**147–158.

Address correspondence to: Myong-Hee Sung, National Cancer Institute, National Institutes of Health, 6130 Executive Blvd. EPN 8146, MSC 7434, Bethesda, MD 20892. E-mail: sungm@mail.nih.gov

Correction to "In silico simulation of inhibitor drug effects on nuclear factor-κB pathway dynamics"

In the above article [Sung M-H and Simon R (2004) *Mol Pharmacol* **66:**70–75], an error was introduced into Table 1 during the proofreading process. The corrected version of the table appears below.

We regret this error and apologize for any confusion or inconvenience it may have caused.

TABLE 1
AUIC comparison of various therapeutic situations

Inhibitor Type	Maximum Concentration or Activity (% Inhibition)	Binding Affinity	AUIC
		nM	%
A	50 (nM)	6.8[a]	40.3
	150 (nM)	6.8	73.8
	50 (nM)	0.68	67.6
B	50 (nM)	1[a]	20.1
	150 (nM)	1	44.7
	50 (nM)	0.1	48.2
	60 (%)	N/A	19.6
Bortezomib	100 (%)	N/A	39.9

[a] These values are from the original assumption about binding affinities of inhibitor A and B.